Surface roughness and conductivity of thin Ag films

E. Z. Luo, S. Heun, M. Kennedy, J. Wollschläger, and M. Henzler
Institut für Festkörperphysik, Universität Hannover, Appelstrasse 2, D-30167 Hannover, Germany
(Received 19 October 1993)

The diffuse scattering of conduction electrons at a rough surface has a considerable contribution to the resistivity of thin films, which is well known as the classical size effect. We have separated this contribution from other scattering mechanisms such as the phonon and bulk defect scattering by the following procedure: Silver was deposited at low temperatures (≈ 130 K) onto a well-annealed relatively thick silver base layer (≈ 24 nm), which has been deposited onto a Si(111)-7×7 substrate. During deposition the resistivity of the thin film was measured *in situ*, and afterwards the surface roughness was determined quantitatively with profile analysis of low-energy electron diffraction. An increase of both resistivity and surface roughness was observed. Such an increase of the measured resistivity must be due to the increase of surface roughness because there was no change in temperature or concentration of bulk defects. With the measured surface roughness we are able to evaluate the additional resistivity without any free parameters. The experiment reveals excellent agreement with the theoretical predictions.

I. INTRODUCTION

It has been known for a long time that surface diffuse scattering has a considerable contribution to the resistivity of a thin film if its thickness is smaller or comparable with the mean-free-path l of the conduction electrons in this film. This effect is well known as the classical size effect and was studied by Fuchs in 1938,[1] who, using Boltzmann's transport theory, concluded that the resistivity of a thin film with thickness D is given by the following form:

$$\rho(D)=\rho_\infty+\frac{3}{8D}l_\infty\rho_\infty(1-p), \quad 0\le p\le 1 \tag{1}$$

for $D \gg l_\infty$. Here l_∞ is defined as the mean-free path of the conduction electrons in the limit $D\to\infty$. In (1), ρ_∞ and l_∞ are material constants and p is a phenomenological parameter, which is called the specularity parameter and describes the strength of diffuse scattering of conduction electrons at the surface-vacuum interface and at the interface to the substrate of the thin film. According to this theory, a fraction $(1-p)$ of the conduction electrons is scattered diffusively at the surfaces of the thin film, and thus, gives rise to an enhanced resistivity. Since then a number of extensions of Fuchs's theory and other models have been developed,[2-6] all of which conclude that the resistivity of thin films is influenced by the surface morphology, which is characterized by vertical and lateral surface roughness. The results of these models differ from author to author. Besides the theoretical progress on this problem, a wide variety of experiments have also been reported.[7-12] Most of them, however, use simply the specularity parameter p as a free parameter to fit their experimental results, according to Eq. (1). Such a fit does not always work. For instance, in some cases more than one parameter or negative values of p were needed, although this does not make sense within Fuchs's theory. In many cases details of the mechanisms of diffuse scattering at the surfaces cannot be derived, because p is only a phenomenological parameter.

For a better understanding a better theory is needed, which uses explicitly the surface topography as given by roughness and its correlation. Such a theory is available.[6] Then, for the same film, the structural and the electrical data have to be measured. Data for epitaxial Ag films will be presented in this paper. Since the surface roughness has been modified by Ag deposition continuously and the roughness and resistivity have been measured, a quantitative description of roughness scattering is now possible without any fitting parameter.

After a brief description of experimental arrangements in Sec. II, the theoretical background of surface-roughness scattering and the principles of the surface-roughness determination using spot-profile analysis–low-energy electron diffraction (SPA-LEED) will be given in Sec. III. In Sec. IV, the results of both measurements and the comparison with theory will be presented. Discussions and some perspectives will be given in Sec. V.

II. EXPERIMENTS

The experiments of conductivity and surface-roughness measurements were carried out in separate UHV systems, both with a base pressure less than 4×10^{-11} mbar. For the conductivity measurements, the substrates are squares of Si(111) wafers ($\rho=6000$ Ω cm) with contact areas in the corners and notches on each side (see Fig. 1). The conductance is measured and evaluated according to van der Pauw.[13] Due to Au doping ($10^{16}/\mathrm{cm}^3$), the resistance is higher than 20 MΩ at temperatures below $T=50$ K. The crystal was heated in UHV up to 1400 K in order to form a clean, step-free surface with 7×7 superstructure with sharp LEED spots in the center portion of the sample. To ensure good Ohmic contact between the Mo contact areas and even very thin Ag films, 20 monolayers (ML's) of Ag were deposited onto the whole sample and removed only from the center portion of the sample by

 ©1994 The American Physical Society

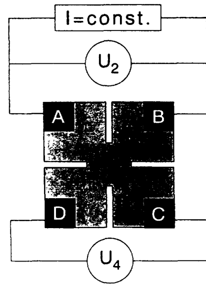

FIG. 1. Geometry of the sample and contact arrangement as used for the conductance measurement.

moderate heating. After this procedure, neither Ag nor Mo were detectable on the center portion of the sample by means of Auger electron spectroscopy. Just a small trace of carbon (< 1%) was detectable. So, the thin films could be deposited onto clean Si(111)-7×7 and contacted by the Ag on the contact areas. The film thickness was monitored by a quartz microbalance, which has been calibrated by comparing the measured temperature coefficient of the resistivity of thick Ag films (> 100 ML) with bulk literature data. The calibration was also checked using *ex situ* x-ray diffraction. In order to measure separately the effect due to roughness scattering, first a thick film ($D \approx 24$ nm) was deposited at 90 K and annealed for optimum conductance. The changes of resistivity, as measured during further deposition at low temperatures (85–200 K), are then just due to the increased roughness at the surface.

The measurements of surface roughness were carried out in another UHV system. The LEED data were taken with the SPA-LEED system described in detail in Refs. 14 and 15. Due to the high-transfer width (200 nm) over a broad energy range, roughness and correlation length may be measured with high precision. Furthermore, the chamber is equipped with an Auger system with a cylindrical mirror analyzer. The samples could be cooled down to 130 K by liquid nitrogen and heated up to 1500 K by electron bombardment. The preparation of the Si substrate and the Ag film has been the same as for the resistivity measurements.

III. THEORETICAL ASPECTS

A. Surface-roughness scattering of conduction electrons

There are many theoretical models dealing with this problem.[2–6] Although there are some differences among these theoretical models, the final results differ not very much from each other (at least for the extra resistivity due to surface-roughness scattering). Surface-roughness resistivity can be understood in the way that conduction electrons are submitted to additional scattering at the rough surface due to the perturbation potential at the atomic steps.

A schematic view of a typical rough surface is shown in Fig. 2. There are two ways to characterize quantitatively a rough surface.

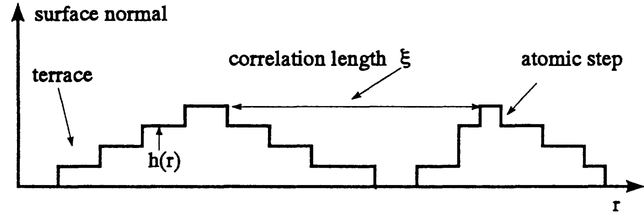

FIG. 2. Schematic cross section of a rough surface.

It may be described in a discrete way by the vertical surface roughness Δ [or layer distribution $P(h)$] and the mean terrace length $\langle L \rangle$ [or the terrace-length distribution $P(L)$]. The existing transport theories concerning the surface-roughness scattering describe the rough surface by the height-difference function $H(r)$ defined as

$$H(\mathbf{r}) \equiv \langle [h(\mathbf{r}+\mathbf{r}')-h(\mathbf{r}')]^2 \rangle = \sum_h h^2 C(\mathbf{r},h) \ , \qquad (2)$$

where $h(\mathbf{r})$ is the vertical position of the surface atom at lateral position $\mathbf{r}$ related to a reference plane, as shown in Fig. 2. In Eq. (2), the angular brackets $\langle \ \rangle$ denote averaging with respect to $\mathbf{r}'$, and $C(\mathbf{r},h)$ is the pair correlation for height difference h.

It is easy to rewrite Eq. (2) by expanding it as

$$H(\mathbf{r}) = 2\Delta^2 - 2\langle h(\mathbf{r}+\mathbf{r}')h(\mathbf{r}) \rangle \ . \qquad (2a)$$

The first term on the right side of Eq. (2a) is the vertical roughness Δ (one point average, or asperity height) defined as

$$\Delta^2 \equiv \langle h^2(\mathbf{r}) \rangle - \langle h(\mathbf{r}) \rangle^2 \qquad (3)$$

and the second term of Eq. (2a) describes the lateral height-height correlation (two points average), which depends on $\mathbf{r}$ and may be described in terms of a correlation length ξ through the height-height correlation function $g(\mathbf{r}/\xi)$ defined as

$$\langle h(\mathbf{r}+\mathbf{r}')h(\mathbf{r}) \rangle \equiv \Delta^2 g(\mathbf{r}/\xi) = \Delta^2 \exp(-r/\xi) \ . \qquad (4)$$

According to Eqs. (2)–(4), a rough surface is described by the two parameters Δ (roughness) and ξ (correlation length) concerning the vertical and lateral disorder, respectively. The correlation function $g(\mathbf{r}/\xi)$ is frequently approximated by a Gaussian or exponential function. Here, only the exponential autocorrelation form is used due to a better fit to the experiment.

Based on the formalisms of a force-balance equation, recently Kaser and Gerlach[6] have shown that for thin-metal films the resistivity ρ_{sr} due to the surface-roughness scattering can be quantitatively expressed as

$$\lim_{D_{k_f} \to \infty} \rho_{sr} = \frac{9\pi\hbar\Delta^2}{2e^2 D} F(k_f \xi) \ , \qquad (5)$$

if the thickness D of the film is thick enough to neglect the quantum size effects. In Eq. (5), k_f is the Fermi wave vector, e is the electron charge, and $\hbar$ is Planck's con-

stant. The function $F(k_f\xi)$ in Eq. (5) is a well-defined function and can be calculated numerically. For very large and very small $k_f\xi$ one gets

$$F(k_f\xi)\approx 0.666/k_f\xi \quad \text{for } k_f\xi \gg 5$$
$$=\frac{4\pi}{45}(k_f\xi)^2 \quad \text{for } k_f\xi \ll 2 \; . \tag{6}$$

In deriving Eq. (5), it is assumed that the potential at the surface is infinitely high. The corrections of $F(k_f\xi)$ for a finite potential, however, are very small.[6]

B. Spot-profile analysis

Surface roughness Δ has been derived from SPA-LEED of the 00 beam, as described in the literature.[14–18] A stepped surface, as shown in Fig. 2, produces a spot profile consisting of a central spike $G_0(S)$ and a shoulder G_{diff}. The function $G_0(S)$ varies as

$$G_0(S)=\exp\{-2\Delta'^2[1-\cos(2\pi S)]\} \; , \tag{7}$$

with scattering phase $S=dk_\perp/2\pi$. Here $\Delta'=\Delta/d$ is the surface roughness in units of the layer spacing d, and $k_\perp$ is the normal component of the scattering vector. Experimentally $G_0(S)$ is given by the ratio of the integrated central-spike intensity to the integrated total intensity $I_{\text{central}}/I_{\text{total}}$.[18] Close to the out-of-phase conditions ($S=n+\frac{1}{2}$, n an integer), the diffuse shoulder for a geometric terrace-length distribution is given by

$$G_{\text{diff}}(k_\parallel)\propto\frac{1}{[\kappa^2+(ak_\parallel)^2]^{3/2}} \tag{8}$$

with

$$\kappa=\frac{[1-\cos(2\pi S)]}{\langle L\rangle} \; , \tag{9}$$

where a is the atomic-row distance in the Ag(111) plane ($a=0.289$ nm) and $\langle L\rangle$ the average terrace length, which is given in atomic units. The half-width at the out-of-phase condition provides directly the average terrace length $\langle L\rangle$ via $\kappa=2/\langle L\rangle$. Since the experimental profiles are well fitted with the Lorentzian shape [Eq. (8)], the terrace-width distribution has to be geometric. A Gaussian distribution does not fit the experimental curve.

C. Evaluation of the correlation length from LEED experiments

The previous sections have shown that on one hand SPA-LEED characterizes the surface morphology by the asperity height Δ and the average terrace length $\langle L\rangle$. On the other hand, besides the asperity height, the correlation length ξ is the correct quantity to describe the resistivity of thin films. In this section, we will present how the correlation length ξ can be obtained from SPA-LEED data taken at the out-of-phase condition.

For simplicity reasons, it is useful to study the phase correlation

$$\Phi(\mathbf{r},S)=\langle\exp\{ik_\perp[h(\mathbf{r},\mathbf{r}')-h(\mathbf{r}')]\}\rangle$$
$$=\sum_h C(\mathbf{r},h)\exp(ik_\perp h) \; . \tag{10}$$

Here $C(\mathbf{r},h)$ denotes the pair correlation [cf. Eq. (2)]. The phase correlation is just the two-dimensional Fourier transform of the spot profile for the scattering phase S. Thus, a profile which is split into a central spike and a Lorentzian shoulder (cf. Sec. III B) transforms into a phase correlation:

$$\phi_{\text{LEED}}(\mathbf{r},S)=G_0+(1-G_0)\exp(-\kappa\mathbf{r}) \quad \text{with } \kappa=\kappa(S) \; . \tag{11}$$

Here the constant part G_0 is due to the central spike, and the exponential part due to the shoulder.

In order to combine the phase correlation $\Phi(\mathbf{r},S)$ with the height-difference function $H(\mathbf{r})$, one has to assume a special form of the pair correlation with respect to the height difference h. For a rough surface with many levels ($\Delta\gg d$), it is reasonable to suppose an exponential form:

$$C(\mathbf{r},h)\propto\exp(-\alpha|h|) \quad \text{with } \alpha=\alpha(\mathbf{r}) \; . \tag{12}$$

Inserting this pair correlation into Eqs. (2) and (10), we obtain the phase correlation

$$\Phi(\mathbf{r},S)=[1+H(\mathbf{r})\{1-\cos(2\pi S)\}]^{-1} \tag{13}$$

with the height-difference function [cf. Eqs. (2)–(4)]

$$H(\mathbf{r})=2\Delta^2[1-\exp(-\mathbf{r}/\xi)] \; . \tag{13a}$$

This phase correlation does not match exactly the phase correlation from LEED experiments. However, we are not interested in the exact form of the correlation function, we want to compare correlation and terrace lengths. Thus, we have to use some "fitting criterion" to compare both phase correlations. For this reason we use the criterion

$$\partial_r\Phi(\mathbf{r},S)=\partial_r\phi_{\text{LEED}}(\mathbf{r},S) \quad \text{at } \mathbf{r}=\mathbf{0} \; . \tag{14}$$

This matching condition shows that the half-width depends via

$$\kappa(S)=\frac{2\Delta'^2[1-\cos(2\pi S)]}{\xi[1-G_0(S)]} \tag{15}$$

on the scattering phase S, the asperity height Δ', and the correlation length ξ. On the other hand, we have seen in Sec. III B [Eq. (9)] that the half-width depends only on the average terrace length $\langle L\rangle$. Comparing Eq. (15) with Eq. (9) for the out-of-phase condition ($S=n+\frac{1}{2}$), we obtain that the correlation length ξ scales with both the average terrace length $\langle L\rangle$ and the asperity height Δ' via

$$\xi=2\Delta'^2\langle L\rangle \; . \tag{16}$$

Here one has neglected the variation of the central spike $G_0\approx 0$, since it decreases rapidly for rough surfaces at the out-of-phase condition [cf. Eq. (7)]. Equation (16) shows that one needs both information from SPA-LEED: the average terrace length (obtained from the half-width of the shoulder at the out-of-phase condition) and the asperity height (obtained from the variation of the central spike) to evaluate the correlation length ξ involved in the surface scattering of conduction electrons.

IV. RESULTS

A. Characterization of well annealed, epitaxial films as substrates

Silver grows well epitaxially on Si(111) with (111) orientation; this feature is independent of film thickness and growth temperature.[19,20] Figure 3 shows a LEED pattern taken from a 100-ML-thick Ag film deposited at room temperature, which shows a sixfold symmetry of the {10} spots. This symmetry is independent of the electron energy, which means that the film has stacking faults.[21] In order to characterize the surface morphology quantitatively, one-dimensional profiles have been measured and analyzed. The dependence of full width at half maximum (FWHM) of the (00) beam on the scattering phase S is illustrated in Fig. 4, which shows that besides a small oscillation, the FWHM increases linearly with S. The linear increase of FWHM results directly from a mosaic spread. The (111) axis of Ag mosaics fluctuates with respect to the (111) axis of the Si substrate. These fluctuations lead to an isotropic broadening of the spots. From the slope of this linear increase of FWHM, the standard variation of the angular distribution of mosaic spread (denoted as mean mosaic angle Θ below) can be derived.[16] The small oscillation of the FWHM with S is due to atomic steps on the surface.[16-18] Both the mosaic angle and the atomic-step density can be decreased by annealing. After annealing at 450 K, the typical value of the mean mosaic angle Θ is about 0.12° and the mean terrace length is about 70 atomic distances (≈ 20 nm). Both parameters may vary a bit with deposition conditions.[19]

The resistivity of the thick ($D \geq 20$ ML) epitaxial Ag films is well described by a residual resistance at low temperatures and a linear increase with temperature. The residual resistance is due to bulk and interface defects. After deposition at low temperatures ($T < 100$ K) and annealing (up to 450 K), the residual resistance is proportional to the inverse of thickness, revealing a strong scattering at the interface.[22,23] The resistivity of base layers is, therefore, given by the classical size effect.

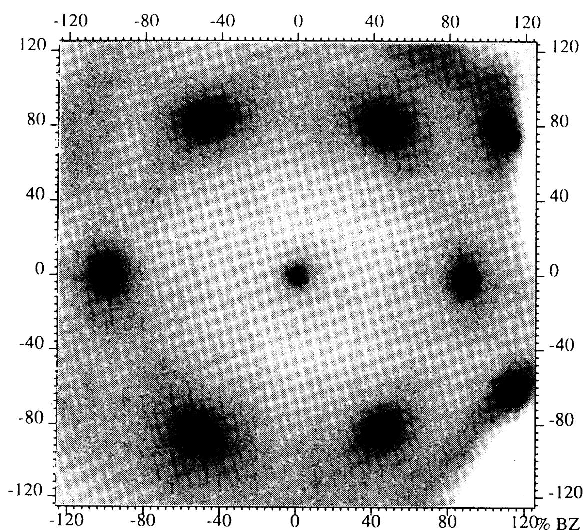

FIG. 3. LEED pattern from thick Ag film (100 ML$\approx$24 nm) deposited on Si(111)-7×7 at room temperature. The central spot is the (00) beam.

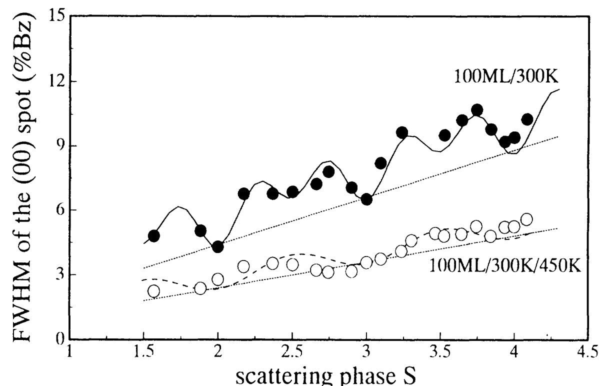

FIG. 4. Variation of the FWHM of the (00) spot of a 100-ML-thick silver base layer with the scattering phase S after deposition at room temperature (upper curve) and after annealing at 450 K (lower curve). The FWHM has been scaled in units of the scattering vector of the (10) beam of Ag(111).

B. Growth of rough layers at 130 K on well-annealed films

1. *Surface morphology after low-temperature deposition*

After deposition of Ag at 130 K onto a well-annealed film, the spot profiles show drastic variations. For in-phase condition (neighboring terraces scatter in phase) no change is observed. It is therefore concluded that all deposited atoms are in exact lattice sites, pointing to perfect epitaxy.[18] For all other phase conditions, the profile consists of a central spike and a shoulder, which is typical for a stepped surface (Fig. 5).[18] The separation into central spike and shoulder was possible up to 3.5 ML. The shape of the central spike before and after deposition is given by the instrumental broadening due to the mosaic structure of the film (Fig. 4). The fraction G_0 of intensity in the

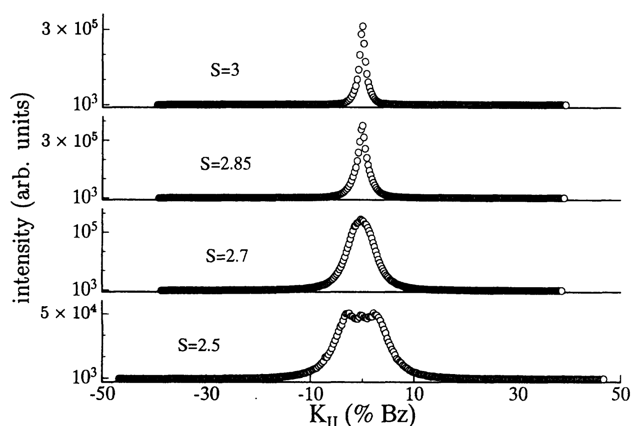

FIG. 5. LEED profiles for different scattering conditions after deposition of 1-ML Ag at 130 K on a well-annealed silver film.

central spike out of the total spot intensity as a function of scattering phase S provides the vertical distribution as given by the roughness Δ' (Fig. 6).[18] The roughness Δ' for coverage up to 3.5 ML is plotted in a quadratic scale in Fig. 7. It clearly reveals a dependence of $\Delta'^2=\theta$, which indicates that all atoms stay in that level where they have been deposited (random mode[24]). The vertical distribution is, therefore, given by the Poisson distribution. There has to be a barrier at step edges, so that crossing of the edge is unlikely. Nevertheless, diffusion on terraces may be possible.

This diffusion is derived from the half-width of the shoulder. As seen in Fig. 5, the shoulder is like a ring with a maximum (at k_r). The cross section of the ring may be described by the superposition of two Lorentzians with parameter κ [as in Eq. (8)] and shifted by $\pm k_r$ from center position. The FWHM of the Lorentzians and the maximum position k_r vary with scattering phase as shown in Fig. 8. From the values at out-of-phase condition, the average terrace length $\langle L \rangle$ and the standard deviation of its distribution are derived from[25]

$$\kappa a \langle L \rangle = \pi^2 \left[\frac{\sigma}{\langle L \rangle} \right]^2 ,$$
$$k_r a \langle L \rangle = \pi \left\{ 1 - \frac{\pi^2}{6} \left[\frac{\sigma}{\langle L \rangle} \right]^4 \right\} . \tag{17}$$

The average terrace width $\langle L \rangle$ as derived from Eq. (17) for coverages up to 3.5 ML is shown in Fig. 9. A least-squares fit (solid line in Fig. 9) is given by $\langle L \rangle = 12.5\theta^{-2/3}$. Without diffusion on terraces, this value should be around 2 for all coverages. Therefore, a considerable diffusion on terraces takes place, whereas simultaneously, the crossing of step edges is negligible. A quantitative evaluation of the barrier for surface diffusion is in preparation.[19]

So far the surface morphology has been quantitatively determined in the language of asperity height Δ and mean terrace length $\langle L \rangle$. However, Eq. (5) indicates that the surface-roughness resistivity depends on Δ and ξ. The second parameter is given by $\langle L \rangle$ and Δ according

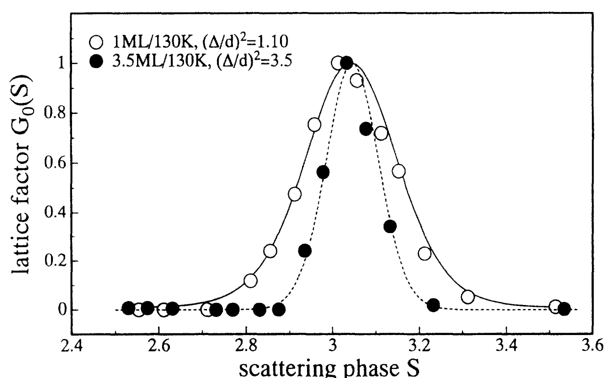

FIG. 6. Variation of $G_0(S)$ (the ratio of the integrated central spike intensity to the integrated total intensity) with the scattering phase S after deposition of 1 ML (open circles) and 3.5 ML (filled circles) of silver at 130 K. The asperity height Δ has been obtained according to Eq. (7).

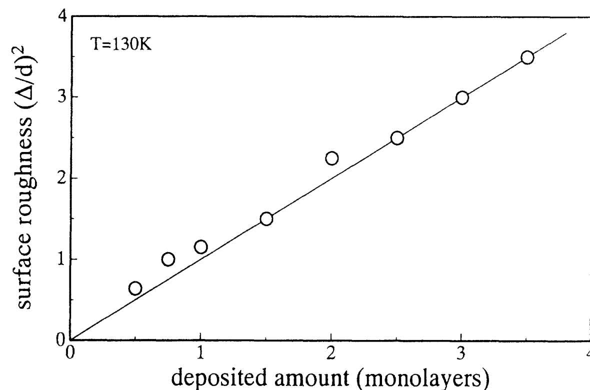

FIG. 7. The coverage dependence of the asperity height $(\Delta/d)^2$ with coverage θ, which shows exactly $\Delta^2=\theta$ (straight line) at a deposition temperature of 130 K.

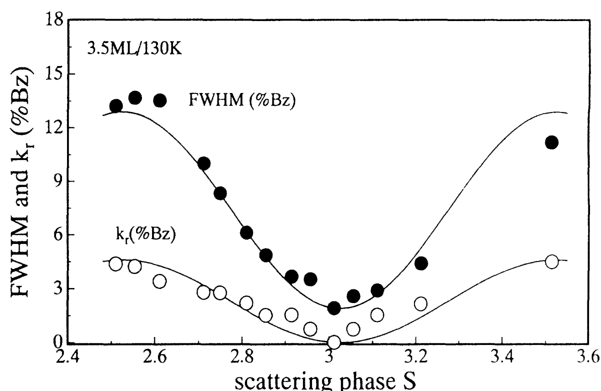

FIG. 8. The variation of the FWHM (filled circles) and radius of maximum k_r (open circles) of the diffuse shoulder of the (00) spot with scattering phase S after deposition of 3.5-ML silver at 130 K.

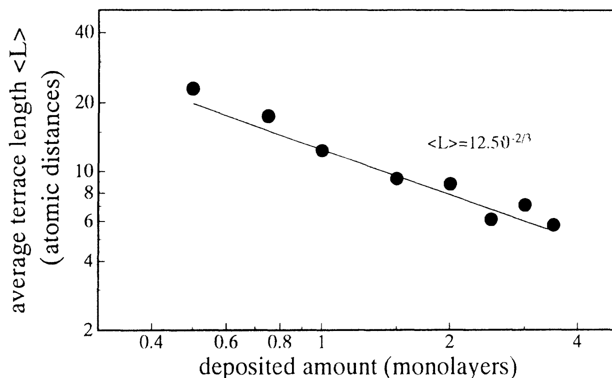

FIG. 9. The coverage dependence of the mean terrace length $\langle L \rangle$ (filled circles) at a deposition temperature of 130 K.

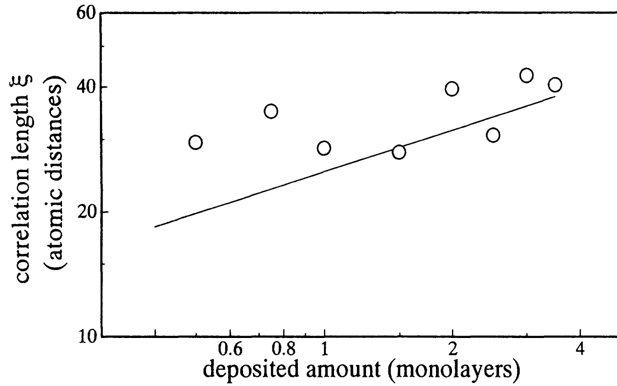

FIG. 10. The correlation length ξ (open circles) calculated using Eq. (16). For the calculation, Δ and $\langle L \rangle$ have been used. The solid line shows the calculated ξ using the power-law dependency of Δ and $\langle L \rangle$.

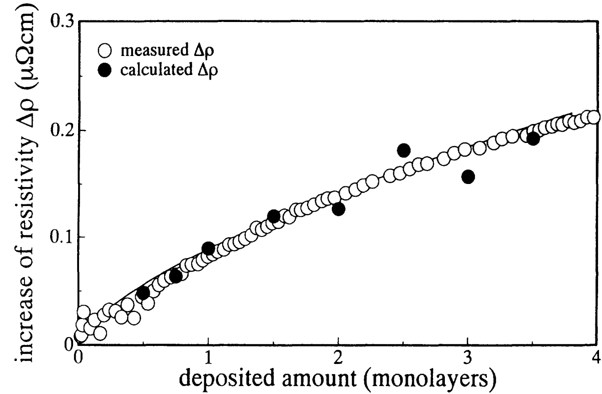

FIG. 11. The measured resistivity change $\Delta\rho$ (open circles) during deposition of additional silver at 130 K on a 116-ML thick well-annealed base Ag layer, and the calculated $\Delta\rho$ using Eqs. (5) and (6), and the measured roughness parameters (filled circles) shown in Figs. 7 and 10, respectively. The solid line is calculated using for ξ the solid line in Fig. 10 and for Δ the solid line in Fig. 7.

to Eq. (16). The results are given in Fig. 10. The solid line in Fig. 10 shows the calculated correlation length ξ with Eq. (16) using the fitted $\Delta'(\theta)$ $[\Delta'(\theta)=\sqrt{\theta}]$ as shown by the solid line in Fig. 7, and $\langle L(\theta)\rangle$ $[\langle L(\theta)\rangle = 12.5\theta^{-2/3}]$ as shown by the solid line in Fig. 9. Figure 10 shows the coverage dependence of the correlation length ξ, which decreases at the beginning of the growth (up to about 0.5 ML, not shown in Fig. 10) and then increases with the coverage. It is easy to understand this feature if we look at the epitaxial growth process. A perfectly smooth surface has an infinite correlation length. For very small coverage, two-dimensional islands are formed and the correlation length is proportional to the mean distance between the adjacent island. As the coverage is increased, the islands density increases also, so the correlation length decreases. If the coverage is further increased, hills and valleys are formed (see Fig. 2), and the correlation length is defined as the mean distance between the adjacent hills and valleys, as shown in Fig. 2. It increases with time (coverage) at the later stage of growth, as predicted by many theoretical studies.[26]

2. *Comparison with the resistivity measurements*

The resistivity measurements have been carried out on a film of 116 ML thickness deposited on Si(111) at 90 K and annealed up to 450 K. During the deposition of the additional Ag at 130 K, the resistivity has been measured *in situ*. An increase $\Delta\rho$ of the resistivity has been observed, shown in Fig. 11 (open circles). This increase is caused by an increase of surface-roughness scattering since the film is epitaxial and there are no other changes of the film morphology besides surface roughness. As discussed above, $\Delta\rho$ is evaluated quantitatively according to Eqs. (5) and (6) with the measured Δ and ξ. Therefore, no free-fitting parameters are left in this calculation. In Fig. 11, the filled circles are the values for $\Delta\rho$ calculated with Eqs. (5) and (6) using the measured surface-roughness data illustrated in Fig. 7 (Δ) and in Fig. 10 (ξ). The solid line in Fig. 11 illustrates the calculated values for $\Delta\rho$ using the power law for Δ and ξ. It can be seen that the evaluation agrees excellently with the measured $\Delta\rho$.

C. Annealing of rough surfaces

It has been shown that low-temperature deposition produces rough surfaces with increasing resistivity. On the other hand, the resistivity of thin films with rough surfaces can be reduced if they are annealed, due to the decrease of surface roughness by annealing. This effect has been checked by the resistivity measurements. Figure 12(a) shows the resistivity during annealing of 0.5-ML Ag deposited at 87 K on a well-annealed Ag film (90 ML). The increase of resistivity due to phonon scattering ($\Delta\rho_T = \alpha T$) has been subtracted, so that only the irreversible changes are plotted. Because the maximum annealing temperature in this case is 300 K, any additional annealing of the starting film (annealed at 450 K) is excluded. Therefore, the decrease of the resistivity is caused by surface smoothing. Nearly the same procedure has also been taken in the SPA-LEED measurements: 0.5-ML Ag was deposited at 130 K and annealed. During annealing LEED profiles have been measured. The FWHM of the (00) spot at the out-of-phase condition ($S = 2.5$, $E = 42.5$ eV) is shown in the inset of Fig. 12(a) with nearly the same decrease as the resistivity. Figure 12(b) provides the same information for $\theta = 2.5$ ML. For rough surfaces ($\Delta \gg 1$), according to Eq. (16), the FWHM at the out-of-phase condition follows approximately the behavior FWHM $\propto \Delta^2/\xi$. With the help of Eqs. (5) and (6), the FWHM reproduces the surface-roughness resistivity, i.e., a decrease of FWHM means a decrease of surface-roughness resistivity. To determine Δ and ξ separately, one has to measure spot profiles for different scattering phases for all annealing temperatures. Those experiments are in progress. The present results, however, are a first approximation.

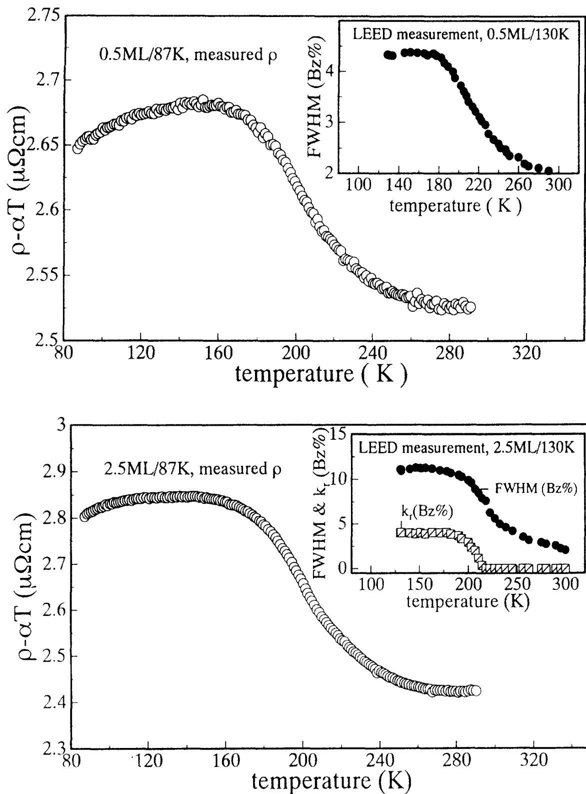

FIG. 12. Resistivity (open circles) and FWHM at out-of-phase condition (filled circles) during annealing of a Ag film with deposition of 0.5 ML (a) and 2.5 ML (b) at 87 K (for resistivity) and at 130 K (for LEED). The reversible variation of resistivity with temperature (αT) has been subtracted. In (b) the radius of the ring maximum k_r is also shown.

V. DISCUSSIONS

The present results show with the measurements of the parameters roughness Δ and correlation length ξ the resistivity increase due to roughness scattering is described quantitatively without any fitting parameter. The following discussion should show some limitations of the approximations used and possible extensions. In this paper the correlation length ξ has been calculated from roughness Δ and average terrace length $\langle L \rangle$, as derived from FWHM at out-of-phase condition. A better way would be to use the FWHM of the shoulder close to in-phase condition (see Fig. 8 for S close to 3). Here the correlation length may be determined directly without using the roughness. So far the measurement close to in phase is less precise, because the shoulder is difficult to separate from the central spike. The accuracy will be improved when better Ag films with less mosaic spread are available. Preliminary experiments using the Si(111)$\sqrt{3}\times\sqrt{3}R\,30°$-Ag as a starting surface are promising.

The theory (see Sec. III A) has been used just in the approximation for large values of $k_f\xi$ in accordance with the experiment, so that the effect of roughness scattering is well described by $\rho_{sr} \propto \Delta'^2/\xi$. With Eq. (17), the resistivity increase ρ_{sr} is simply given by $1/\langle L \rangle$, which is just the density of atomic steps. If each atomic step is considered as an independent scatterer for conduction electrons (a model used by Wißmann[4]), a much simpler model may describe the results. From this theory it is seen that this model only works by chance for large values of $k_f\xi$. On the contrary, resistivity may increase with ξ for sufficiently small values of ξ. Experimentally this may be realized by deposition of Ag at much lower temperatures, so that the average value of $\langle L \rangle$ and the correlation length ξ are much smaller. Another possibility is to use a metal with a smaller k_f (e.g., a semimetal). Those experiments are in preparation.

In the present study, essentially the average terrace length has been used. The spot-profile analysis provides the full terrace-width distribution, which deviates to some extent from the geometric distribution.[19] It will be interesting to see if those details reflect special properties of the resistivity too.

The present study shows that detailed measurements of the surface roughness, including terrace-width distribution, provide a new and efficient way to describe the effect on resistivity without free parameters. Along those lines it should be also possible to describe other effects like magnetoconductance or conductance of very thin films in full detail. Those experiments are in preparation.

ACKNOWLEDGMENTS

Valuable discussions with A. Kaser and E. Gerlach and their permission to use their unpublished theoretical results are gratefully acknowledged. One of us (E.Z.L.) wishes to acknowledge the partial financial support from the Universität Hannover (Graduiertenförderung). The investigations have been supported by the Deutsche Forschungsgemeinschaft and the Volkswagen-Stiftung.

[1]K. Fuchs, Proc. Cambridge Philos. Soc. **34**, 100 (1938).
[2]E. H. Sondheimer, Adv. Phys. **1**, 1 (1952).
[3]S. B. Soffer, J. Appl. Phys. **38**, 1710 (1967); J. R. Sambles, Thin Solid Films **106**, 321 (1983); J. R. Sambles and T. W. Preist, J. Phys. F **12**, 1971 (1982).
[4]P. Wißmann, in *The Electrical Resistivity of Pure and Gas Covered Metal Films*, edited by G. Höhler, Springer Tracts in Modern Physics No. 77 (Springer, Berlin, 1975), p. 1.
[5]K. M. Leung, Phys. Rev. B **30**, 647 (1984).
[6]A. Kaser and E. Gerlach (unpublished).
[7]M. S. P. Lucas, Appl. Phys. Lett. **4**, 73 (1963); Thin Solid Films **170**, 435 (1971).
[8]K. L. Chopra, L. C. Bobb, and M. H. Frnancombe, J. Appl. Phys. **34**, 1699 (1963); K. L. Chopra, Phys. Lett. **15**, 73 (1965).
[9]D. C. Larsen and B. T. Boiko, Appl. Phys. Lett. **5**, 155 (1964).
[10]B. Fischer *et al.*, Z. Phys. B **42**, 349 (1982).
[11]D. Schumacher and D. Stark, Surf. Sci. **123**, 384 (1982).
[12]D. Schumacher, in *Surface Scattering Experiments with Conduction Electrons*, Springer Tracts in Modern Physics No. 128 (Springer, Berlin, 1993), and references therein.

[13]L. J. van der Pauw, Philips Res. Rep. **13**, 1 (1958).
[14]U. Scheithauer, G. Meyer, and M. Henzler, Surf. Sci. **178**, 441 (1986).
[15]Th. Schmidt, Diploma thesis, Universität Hannover, 1990.
[16]M. Henzler, Appl. Surf. Sci. **11/12**, 450 (1982); in *Electron Spectroscopy for Surface Analysis,* edited by H. Ibach (Springer, Berlin, 1977), p. 117.
[17]M. Henzler, in *The Structure of Surfaces II,* edited by J. F. van der Veen and M. A. Van Hove, Springer Series in Surface Science Vol. 11 (Springer, Berlin, 1988).
[18]J. Wollschläger, J. Falta, and M. Henzler, Appl. Phys. A **50**, 57 (1990).
[19]E. Z. Luo, J. Wollschläger, F. Wegner, and M. Henzler (unpublished).
[20]E. Z. Luo, D. Thieking, and M. Henzler (unpublished).
[21](111) surface of a perfect fcc crystal has threefold symmetry, which should in turn produce a threefold symmetrical LEED pattern.
[22]S. Heun, *Über die Electrische Leitfähigkeit Ultradünner Filme aus Ag, Pb, und Au auf Si(111)* (Fortschritt-Berichte, Reihe 9, Nr. 159 VDI Verlag, Düsseldorf, 1993); see also R. Schad, S. Heun, T. Heidenblut, and M. Henzler, Phys. Rev. B **45**, 11 430 (1992); Appl. Phys. A **55**, 231 (1992); S. Heun, J. Bange, R. Schad, and M. Henzler, J. Phys. Condens. Matter **5**, 2913 (1993).
[23]M. Kennedy, Diploma thesis, Universität Hannover, 1993.
[24]M. Henzler, M. Horn von Hoegen, and U. Köhler, in *Festkörperprobleme/Advances in Solid State Physics* (Vieweg, Braunschweig/Wiesbaden, 1992), p. 333.
[25]J. Wollschläger and M. Henzler (unpublished).
[26]See, e.g., J. Villain, J. Phys. I **1**, 19 (1991).

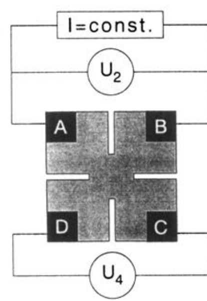

FIG. 1. Geometry of the sample and contact arrangement as used for the conductance measurement.

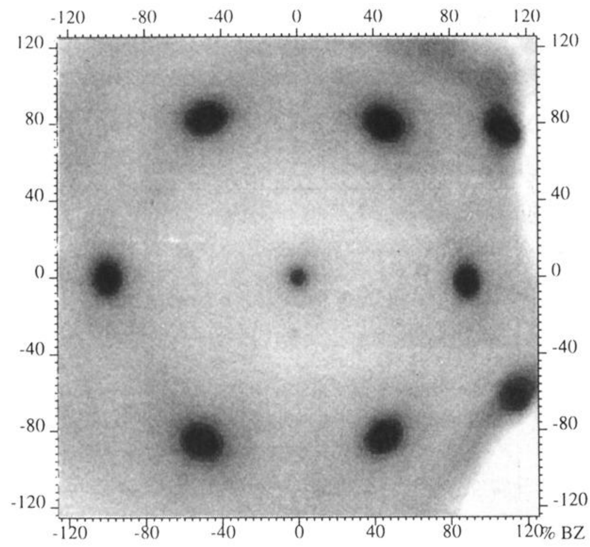

FIG. 3. LEED pattern from thick Ag film (100 ML ≈ 24 nm) deposited on Si(111)-7×7 at room temperature. The central spot is the (00) beam.